Research Article | Vol. 14, No. 7 / 1 Jul 2023 / Biomedical Optics Express 3584
Biomedical Optics EXPRESS

In-vitro quantitative measurement and analysis of the photosensitivity of cells to a weak pulse laser

LAN TIAN,[1] MING ZENG,[1] GENG TIAN,[2] AND JINGJING XU[1,*]

[1]School of Microelectronics, Shandong University, Jinan 250100, Shandong, China
[2]School of Life Sciences, Shandong University, Qingdao 266237, Shandong, China
[*]xujj@sdu.edu.cn

Abstract: Light can trigger electrical activity in certain types of cells, and is considered to be a better means of biological regulation than electrical stimulation in the future. Due to the specificity and selectivity of natural cells' photoresponse to optical signals, constructing an applicable method to explore which kinds of cells have photosensitivity and which bands of light could induce its photoresponse most effectively, is of great significance for lights' medical applications. This paper firstly proposed a universal and operable system and corresponding method to quantitatively measure and analyze photosensitivity of cells in vitro to weak pulse laser, which is constructed with Ca^{2+} imaging module, adjustable laser lights module and laser positioning module. With the measurement system and method, the photosensitive effects of the natural spiral ganglion cells (SGCs) of mice are tested systemantically. Then a new photoresponse band of light (453 nm, 300 μs) is found for SGCs, and its minimum threshold is measured as 5.3 mJ/cm^2. The results verify that the proposed method is applicable to screen the cells with photosensitive response, as well as to measure and analyze the working optical parameters, thus is beneficial for the optical biophysics and photobiology.

1. Introduction

Recently, light has been considered to be a more precise stimulation method to replace electrical stimulation in terms of reconstructing and regulating nerve conduction [1,2], due to its unique advantages in regulating neural activity, such as the non-contact interactions [3,4] and the excellent spatial selectivity [5–7], which enable the stimuli optical signals to be concentrated into micron-scale light spots [8,9]. The study of light-regulated neural activity has gradually become a research hotspot [10–12].

The physiological basis of light-controlled neural regulation technology is that some kinds of natural biological cells have photosensitivity. Studies have found that the activities of cells in the nature can be regulated by time-accurate, fast-changing, and non-invasive optical signals [5]. One mechanism originates from the photosensitive proteins having ability to rapidly form photocurrent and cause a depolarizing electrophysiological reaction in cells, which is the foundation of optogenetics [13]. Besides, when light acts on certain types of natural cells without photosensitive proteins, multiple indistinguishable photoresponses, such as photothermal, optomechanical, and photochemical effects, play roles to induce electrical impulses and/or other biochemical reactions like calcium activities [14–16].

Especially, the light-regulation study on auditory nerves, has been well studied [17,18]. Richter's team in Northwestern University confirmed the potential of infrared light stimulation in modulating auditory nerve activity [4,19,20], and our research group obtained the auditory brainstem responses (ABRs) when stimulate the cochlea of deaf animals using light with a pulse width of 20-200 μs at 980 nm and 810 nm [21,22]. In fact, the wavelength, energy density, pulse width and repetition (frequency) used on the natural spiral ganglion cells (SGCs) of

#494620 https://doi.org/10.1364/BOE.494620
Journal © 2023 Received 2 May 2023; revised 5 Jun 2023; accepted 13 Jun 2023; published 23 Jun 2023

Biomedical Optics EXPRESS

mice in different experimental conditions are quite different [2,18,23]. One possible reason is that the experimental conditions are usually different in different studies. Besides, studies on light-stimulated natural auditory nerves are mostly carried out in vivo, in which light-induced neural activities result from the complex effects between light and multi-tissues like auditory nerve cells, other cells and surrounding internal environment [14]. Above all, the characteristics of photosensitivity are dependent on the parameters of optical signals due to the specificity and selectivity of cell photosensitivity to the stimulus. However, there is no widely applicable calibration or measurement method to analyze and detect whether a target cell has a photosensitive effect, or which bands of light could induce its photoresponse most effectively. Existing methods are limited to the expression verification of photosensitive structures or components, and do not have quick searching or screening abilities.

With the continuous in-depth research of cell photosensitive effects and optogenetics, a multi-spectral and highly operable measurement method for a cellular specific photosensitive effect is urgently needed to accelerate studies on the discovery of specific photosensitive effects of natural cells and the monitoring of the working status of a photosensitive effect in optogenetics, which is also of great significance for the development of photoregulation technology.

Here, we propose a real-time and calcium imaging-based measurement system and method, to explore in vitro which kinds of cells have photosensitivity and which bands of light could induce the photoresponse most effectively. It is applicable to any natural cells, no longer limited to transgenic cells. And any bands (visible and invisible) of optical signals potential to induce cellular photosensitivity effects can be explored. As a result, it is a universal and highly operable system/method, and can implement quantitative and positioning analysis on the photosensitivity of target cells. With the method, the response characteristics of mouse SGCs under the irradiation with different wavelengths were explored and a new photoresponse band is found for them.

2. Materials and methods

2.1. Preconditioning of mouse SGCs

20 mice (C57/BL, 7 days old, male or female) from Jinan Pengyue Laboratory Animal Breeding Co. Ltd. were selected and decapitated. Then, the SGCs in the cochlear shaft were taken out under a dissecting microscope, digested and separated, and placed in a Petri dish with cell slides for in vitro culture in DMEM-F12 medium for 24 h. The temperature was controlled at 37 °C in the gas environment with 95% air and 5% CO_2. When changing medium, the dishes were rinsed twice with Hank's balanced salt solution (HBSS), which contains a large amount of Ca^{2+} and can maintain cell viability for a short time. Before the experiment, specific fluorescent indicator, Fura-2, which characteristically labels intracellular Ca^{2+}, was added in the dishes to incubate the SGCs for 30-60 min. This study and included experimental procedures were approved by the Institutional Animal Care and Use Committee of Shandong University (approval No. KYLL-2022(ZM)-748). All animal housing and experiments were conducted in strict accordance with the institutional guidelines for care and use of laboratory animals.

2.2. Calcium imaging

Calcium imaging is used here to determine the photoresponse of target cells under different parametric light stimuli, because changes of calcium ion concentration is an important event of neural activity [16,24,25]. Calcium imaging uses a calcium indicator to label intracellular calcium ions and reflects changes in intracellular calcium ion concentration through fluorescence imaging.

In this study, Fura-2, a kind of chemical calcium indicator that can specifically bind to intracellular free calcium ions, was used as the fluorescent indicator for calcium imaging experiments. It exists in the form with acetoxymethyl ester (Fura-2-AM) outside the cell, which

Biomedical Optics EXPRESS

enhances its lipid solubility and facilitates entry into the cell through the membrane. It is hydrolyzed into Fura-2 by esterase in cells, which can be directly combined with free calcium ions. The excitation wavelength is 340 nm for combined Fura-2 and 380 nm for free Fura-2, and their emission spectrum peaks are both around 510 nm. By calculating the ratio of the fluorescence intensities at the two excitation wavelengths, that is, F340/F380, the ratio of calcium-bound Fura-2 to free Fura-2 can be determined, and then the free calcium ion concentration can be calculated using the Eq. (1) proposed by Grynkiewicz [26]:

$$[Ca^{2+}]_i = K_d \times \beta \times (R - R_{min}) / (R_{max} - R) \tag{1}$$

where K_d is the equilibrium dissociation constant in the combination process of Fura-2 and calcium ions, and closely related to temperature, pH value, ion concentration, etc. Its value is 224 here, because the experimental temperature was maintained at 37 °C. β is the ratio of fluorescence intensities at zero calcium and saturated calcium inside cell at 380 nm. R is the ratio of fluorescence intensities at the two excitation wavelengths of 340 nm and 380 nm, that is, F340/F380. R_{min} is the ratio of F340/F380 at zero calcium; and R_{max} is the ratio of F340/F380 at saturated calcium. In general, the value of R_{max}/R_{min} is between 13 and 25.

The excitation light source of fluorescence probe adopts the ultra-high-speed wavelength switching device (American SUTTER Lambda DG-4/DG-5 Plus series) whose wavelength range is 330-700 nm, and the wavelength switching speed can reach 1.2 ms during excitation. In the experiment, 2 ms was set up as the wavelength switching speed. Fluorescent calcium imaging of target cells was acquired by a CCD camera (Roper Cool SNAP Color 5 M, USA). In the process of CCD imaging, the higher the pixel resolution, the lower the image frame rate. Balancing the imaging resolution and the change speed of calcium ion concentration, the imaging speed of 2-5 s was adopted.

2.3. Adjustable pulsed laser system

In order to meet the requirements of adjusting wavelength, pulse width, energy density and other parameters of the test light in light-regulation neural activity, we have developed a light source for test lasers, as shown in Fig. 1. The light source system mainly includes array data controller based on Field Programmable Gate Array (FPGA), laser modulation and driver units, fiber-coupled semiconductor lasers, fiber array and other modules. The parameters of the optical pulse signal can be set by buttons or knobs on the control panel, and converted by FPGA into corresponding digital signals to control digital-to-analog converters (DACs) and laser driver unit, to realize real-time programmable control on laser parameters. The pulse width of optical signal can be adjusted from continuous light to 10 μs, and the pulse repetition rate can reach 10 KHz. The pulse energy of a single optical signal can range from 0 to 3.6 mJ, whose adjustment accuracy can reach 1 μJ/div because of the application of high-precision DAC. The energy density described here refers to the optical energy density in the plane of the cells. The calculation formula is as followings:

$$S_{area} = \pi \times (d \times \tan \sin^{-1} NA)^2 \tag{2}$$

where S_{area} is the area of the circular light spot containing many cells on the Petri dish irradiated by the laser, NA is the numerical aperture of the optical fiber, and d is the average distance between the optical fiber outlet and the irradiated cell surface.

Two lasers with different wavelengths were used in the experiment (810nm: K808DB2RN, BWT Beijing, LTD, China, 453nm: RL455F105-4W, Radium Laser Beijing, China). The adjustable pulsed laser system can be expanded to several or more than a dozen wavelengths according to the experimental requirements. The optical signal in different wavelengths is driven by the unified electronic control module, as detailed in the patent (CN202210789664.5 [27]). The optical signals are drawn from the flange port through the optical fiber. In the experiment,

Biomedical Optics EXPRESS

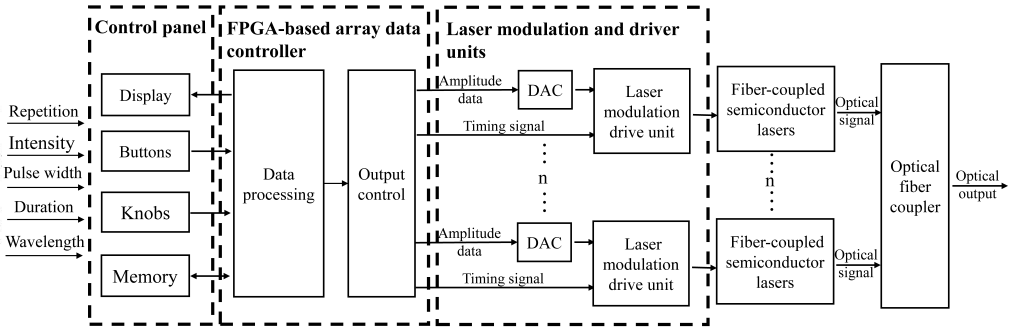

Fig. 1. Parameters adjustable light source system for pulsed lasers.

the location of the optical fiber output remains unchanged, and the optical signals in different wavelengths can be switched freely through the flange port.

2.4. Setup of the photoresponse screening and detecting systems

We have constructed a quantitative screening system for light parameters of stimulus in photoresponse effect of target cells based on calcium imaging. It can dynamically detect the changes of intracellular calcium ion concentration for a large amount of cells, when they are irradiated by lights with different parameters at a reasonable range.

In order to obtain the comparability of measurement results under certain variable, the optical path and other parameters of the system should be kept constant during the measurements. The optical path system shown in Fig. 2. Three different light sources need to be used, one provides test light with adjustable parameters targeted to cells (λ_t), another provides excitation light for fluorescent dyes (λ_e), and the other is the illumination light of microscope (λ_m). In test-light stimulus experiments, the target cells are irradiated by the test light (λ_t) with adjustable parameters, which is emitted by a programmable pulsed laser generator and conducted through optical fiber. The resulting intracellular calcium ion concentration change can be detected by the intensity change of the fluorescence (λ_f), which is excited by excitation light (λ_e) of the fluorescent probe. The microscope illumination light (λ_m) irradiates the target cells, then passes through the dichroic mirror and reaches the eyepiece. During calcium imaging under tested light-stimulation, the microscope illumination light was turned off. The filters, dichroic mirror and lens are used to select light wavelengths and correct optical paths.

Different fluorescent probes have different excitation light and emission light (i.e., fluorescence) wavelengths. To ensure that the imaging results of changes of calcium ion concentration are not interfered by the test light, it must satisfy the interval of more than 10 nm for the wavelength bands of the test light and the excitation and emission lights of the fluorescent probe. In order to separate the light bands in the measurement experiment, a filter set (Chroma, 79001-ET-Fura 2) was used, in which filters in excitation path were ET340x and ET380x, and filters along the fluorescence imaging path were ET510/80 m and ET400lp. The spectrum of the filters and that of the test light are shown in Fig. 3. The area marked in orange in the upper of Fig. 3 is the optional wavelength range of test lights, because the light in this wavelength range can be filtered out by the fluorescence imaging filter set. Here, we choose a blue light (453 nm) and an infrared light (810 nm) as the test lights. It can be seen from the lower part of the diagram that the fluorescence imaging filters can filter out these two kinds of lights

Biomedical Optics EXPRESS

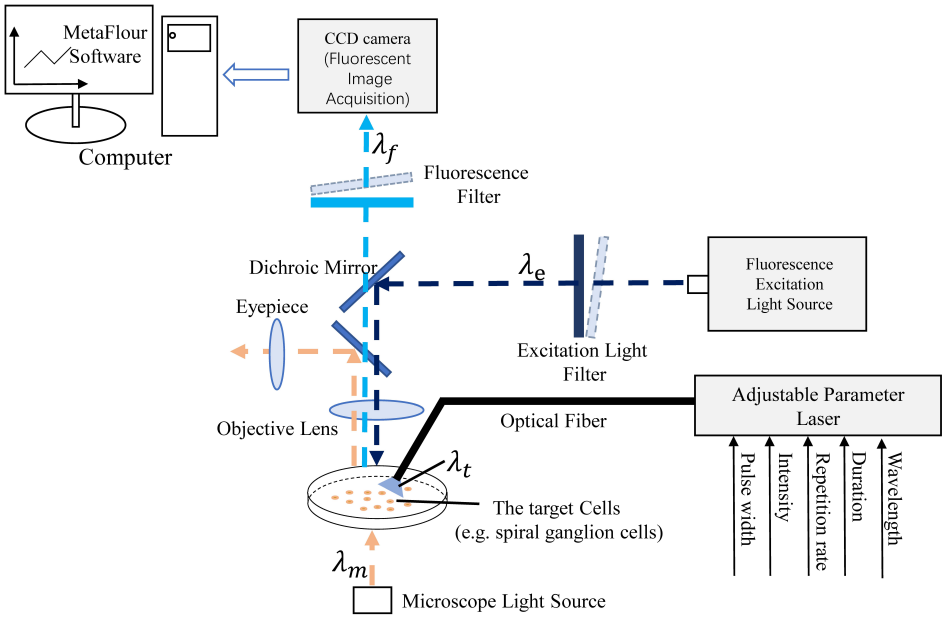

Fig. 2. Schematic diagram of the optical path in the detecting system.

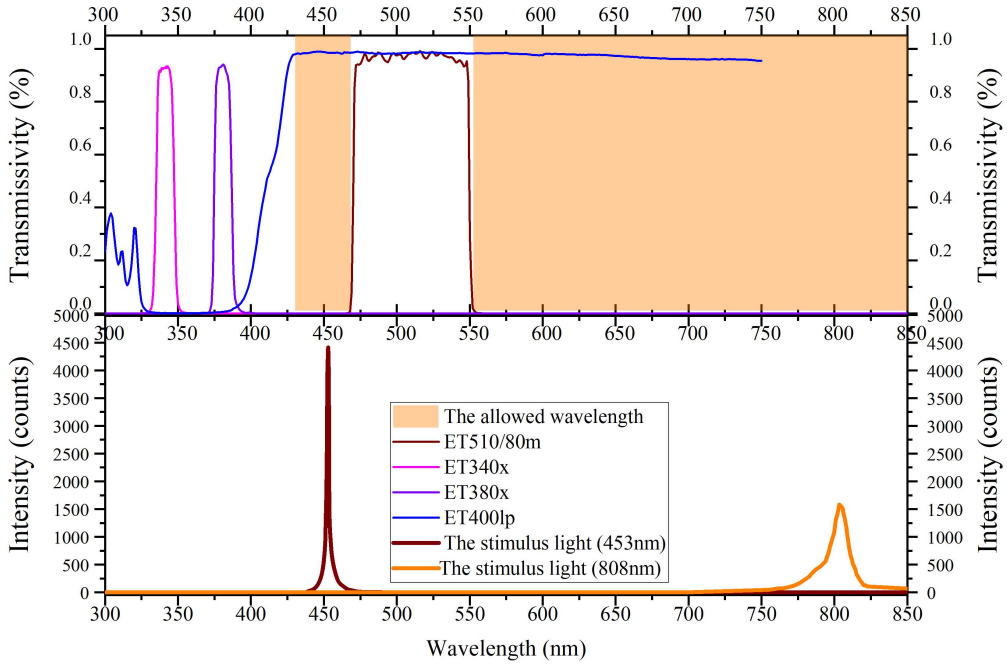

Fig. 3. The optical band of the detection system and the detection results. The spectrum of the filter set and that of the available test lights.

Biomedical Optics EXPRESS

2.5. Data analysis

The measured calcium ion concentration data are divided into two categories, one is the intracellular calcium ion concentration in the resting state, and the other is the intracellular calcium ion concentration at irradiation state, i.e., after light stimulation. The calculation formula is as follows:

$$\rho_m = \frac{(\rho_1 + \cdots + \rho_n)}{n} \tag{3}$$

where ρ_m represents the average value of the fluorescence intensity ratio of F340/F380 in the two states, n represents the number of cells, and ρ_n represents F340/F380 fluorescence intensity ratio of the nth cell.

The tested cells come from the same batch of cultured cells from the same mouse in vitro. The distribution of their intracellular calcium ion concentration is assumed normal. As a result, one-way analysis of variance (ANOVA) was used to analyze the difference of intracellular calcium ion concentration at resting state and irradiation state. If there is significant difference, it means the target cells have photoresponse property. When the one-way ANOVA result in $p < 0.05$, it is believed that there is a significant difference, and the target cells can respond to test light; when $p > 0.05$, we believe that there is no distinguishable difference, and the test light cannot elicit photoresponse on the target cells.

3. Results

3.1. Process of the photoresponse detection on nerve cells in vitro

The process for detecting light regulation on nerve cells in vitro proposed in this paper can be divided into the following steps, as shown in Fig. 4. First, the target cells stripped from the mice are cultured and stained in vitro. The experimental temperature was maintained at 37 °C to mimic the animal's internal environment. Then calcium imaging is performed, and the corresponding Ca^{2+} concentration change curves are collected when target cells are stimulated by test lights with different parameters. Finally, data analysis is performed. In the following, the structure of the detection system and the steps of the detection method are described in detail.

Put the slide with stained and incubated cells into a small dish on the operation table of the calcium imager, and observe the position of the cells and the optical fiber (fiber diameter of 100 µm, NA = 0.22) through the optical microscope (Nikon Eclipse Ti series, Japan). The Field Number (FN) of the microscope system is 22 mm. The objective lens (Nikon CFI Plan Fluor 40X, Japan) of the microscope system was used in the experiments, and its NA is 0.75. The optical fiber port is fixed at a position 1 mm (light spot area is 0.159 mm^2) above the slide by a three-dimensional positioning device. Then, turn off the microscope illumination light, turn on the Fura-2 excitation light, and select cells with complete morphology and appropriate location (closer to the center of light spots) in the fluorescently labeled cell images for subsequent testing experiments. In the cytofluorescence image, the labeled target cells to be tested are shown in Fig. 5(a).

After selecting the target cell, take the light with 453 nm wavelength as an example, set and turn on the laser to irradiate the target cell. The system starts to collect the fluorescence intensity (510 nm) of the fluorescent probe Fura-2 in target cells under the dual-wavelength excitation lasers (340 nm and 380 nm).

Since microsecond-level pulse-width light is usually used in the study of light-induced auditory nerve activity, in the experiment, the pulse width of the selected test lights is all 300 µs. When the SGCs are irradiated with a singular light pulse of 453 nm, the intracellular calcium concentration (InCC) of the part SGCs appeared a significant increase as the light intensity gradually increased from zero, as shown in Fig. 5(b). The measurement results show that the

Biomedical Optics EXPRESS

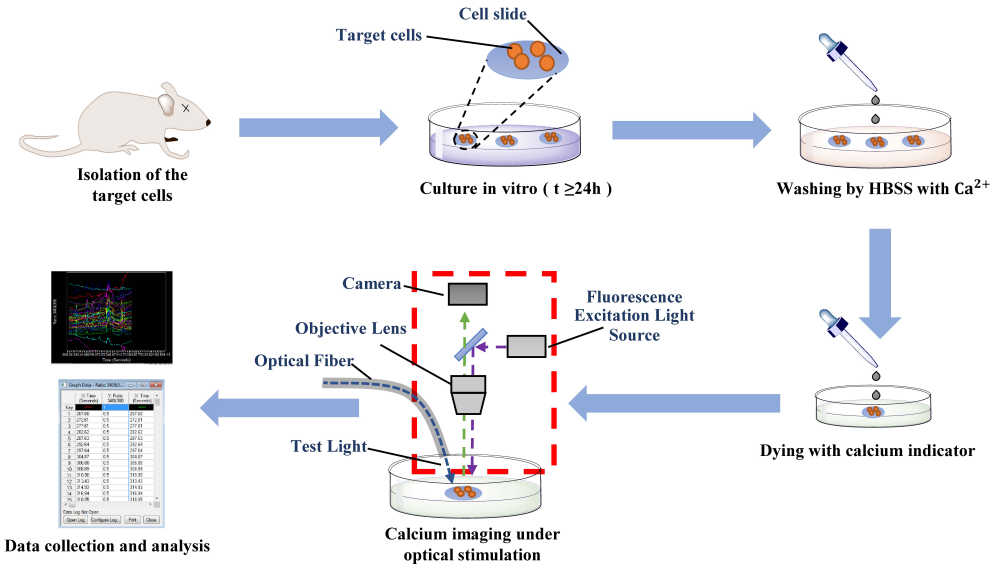

Fig. 4. Flow chart of the method for detecting photoresponse of SGCs in vitro.

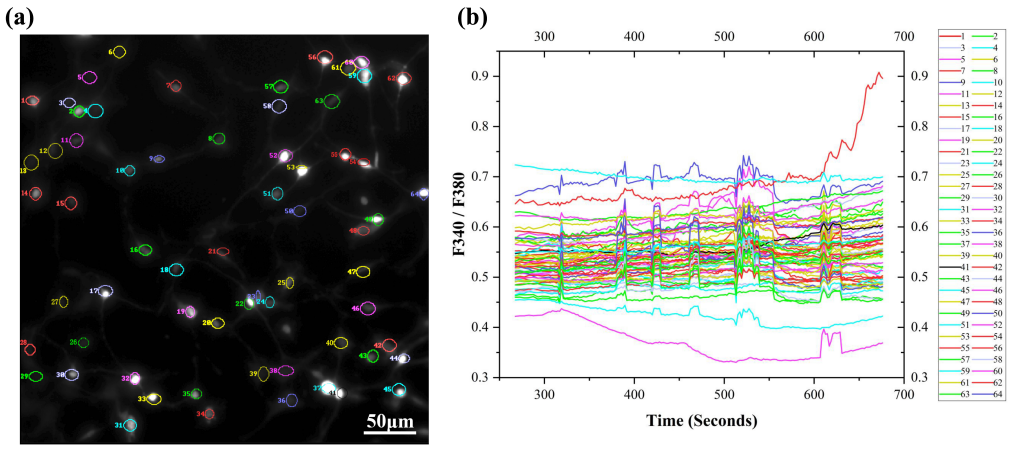

Fig. 5. The target cells and their change curves of intracellular calcium concentration (InCC) under the irritation of 453 nm laser. (a) The target cells labeled by cytofluorescence imaging, (b) The change curve of InCC under 453 nm laser stimulation.

Biomedical Optics EXPRESS

light intensity corresponding to the first significant increase of calcium ions is about 8.4 μJ/pulse, that is, the light intensity threshold of 453 nm for SGCs is 5.3 mJ/cm^2.

3.2. Different photoresponse of SGCs stimulated by 453 nm and 810 nm lights

The statistical results of calcium concentration changes in SGCs (n = 25) in Fig. 5(b) are shown in Fig. 6. In the absence of stimulation lights, the InCC change of SGCs is shown in Fig. 6(a) (time = 0 ~ 45 s). During this time, the fluorescence intensity ratio of F340/F380, that is, the calcium concentration, is low, in which SGCs can be seen at a resting state. When the light intensity exceeds above 8.4 μJ/pulse (5.3 mJ/cm^2), and is successively adjusted to 60.9 μJ/pulse (38.3 mJ/cm^2), 115.2 μJ/pulse (72.4 mJ/cm^2), 170.4 μJ/pulse (107.1 mJ/cm^2), the calcium concentrations of the SGCs all rise and then fall back. Meanwhile, the baseline of the InCC shows a gradual upward trend. The statistical result of significant difference by ANOVA is $p < 0.001$.

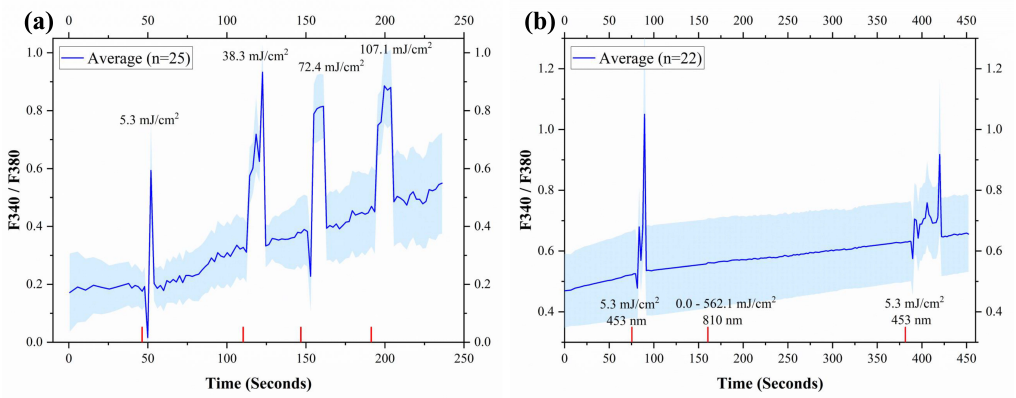

Fig. 6. Changes of ΔCa^{2+} (F340/F380) under the stimulation of test lights. (a) The change curve of F340/F380 when SGCs are irradiated by single-pulse lights (453 nm, 300us) with 5.3 mJ/cm^2, 38.3 mJ/cm^2, 72.4 mJ/cm^2, and 107.1 mJ/cm^2 in turn. The red bars represent the onset time of each single light stimulus, before which there is no test light irradiation. (b) The change curve of F340/F380 when SGCs are stimulated by 453 nm, 810 nm, and 453 nm pulsed lights in turn. Calcium imaging speed is 2-5 s and excitation light switching speed is 2 ms. The light-blue area is the error value distribution range of the corresponding curve. (Data are represented as mean ± SEM)

Biomedical Optics EXPRESS

When stimulated by 453 nm, 810 nm, and 453 nm pulsed lights in turn, the change curve of InCC is shown in Fig. 6(b). It can be found that when the SGCs are stimulated by the 453 nm light, the InCC can be changed both times. When the test light is changed to 810 nm, no significant change in the calcium concentration is found, even though the light intensity is as high as 562.1 mJ/cm^2. The results indicate that the SGCs seem not easy to response to the test light of 810 nm, 300 µs.

Figure 7 further shows the statistical results of changes in calcium concentration of the 25 SGCs before and after light stimulation with different intensities. As shown in Fig. 7(a), as the light intensity increases, the peak of calcium concentration appears a gradual upward trend when the light intensity exceeds 5.3 mJ/cm^2. But the ANOVA results from the baseline, the peak and the peak increment of InCC shown in Fig. 7(b) and (c) suggest that this trend is not significant.

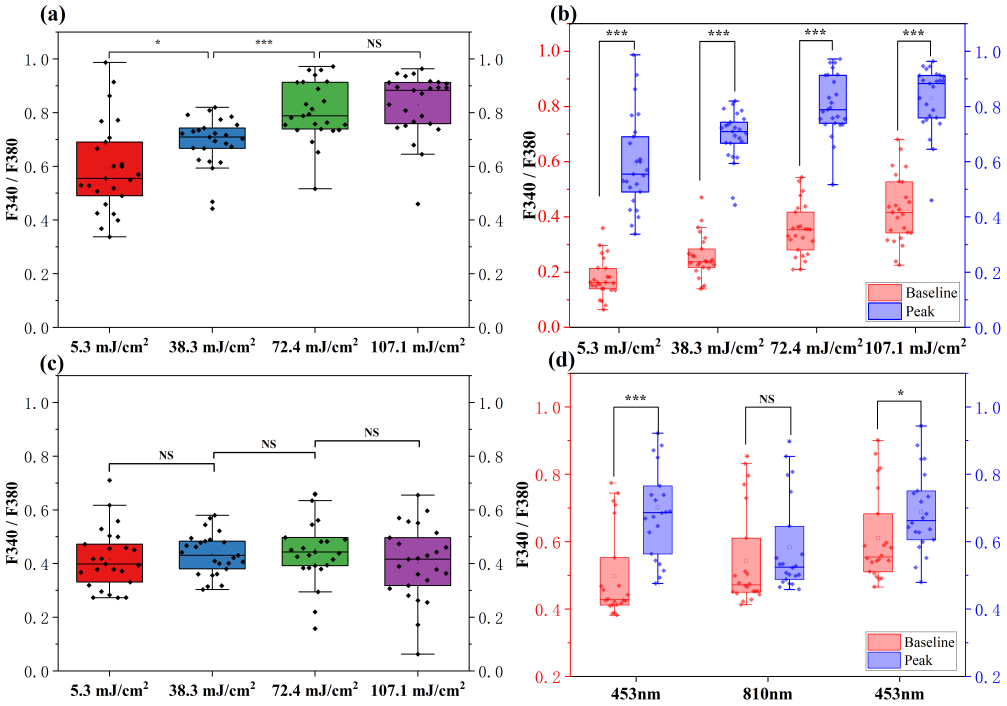

Fig. 7. The statistical results of changes of ΔCa^{2+} (F340/F380) after laser stimulation. (a) The boxplot of the peak of F340/F380 ratio of SGCs stimulated with lights (453 nm) with four different light intensities. (b) The boxplot of the peak of F340/F380 ratio of SGCs under 453 nm lights with four different light intensities and the corresponding ratio in the resting state (baseline). (c) The boxplot of the peak increments of F340/F380 ratio of SGCs under the irradiation of 453 nm lights at different energy densities, that is, the difference between peak and baseline. (d) The boxplot of F340/F380 ratio when stimulated by pulsed lasers of 453 nm, 810 nm, and 453 nm in turn. The black dots are the actual distribution of the fluorescence intensity ratios of the target cells (n = 25). Note: The one-way ANOVA results, $p < 0.001$ (***), $p < 0.01$ (**), $p < 0.05$ (*), $p > 0.05$ (NS).

Figure 7(b) shows the distributions at the resting state and at the excited state by 453 nm light with the red and blue box lines, respectively. And Fig. (c) shows that there was no significant change in the peak increment of the fluorescence intensity ratio change ($p > 0.05$), indicating that the peak increment of calcium concentration does not change with the increase of light

Biomedical Optics EXPRESS

intensity. The increase of the calcium concentration peak may be caused by the increase of the InCC baselines. As a result, the peak increment of calcium concentration does not change with the increase of light intensity.

Figure 7(d) illustrates the statistical results of the significant changes in the InCC of SGCs caused by two 453 nm light stimulations in Fig. 6(b), showing $p < 0.001$ at the first time and $p < 0.05$ for the second time, and that caused by 810 nm light, showing $p > 0.05$. It proves from a statistical viewpoint that the 810 nm laser of 300 µs cannot induce changes of the Ca^{2+} concentration in the SGCs.

4. Discussion

4.1. Reliability of the developed photosensitivity measurement and analysis method/system for cells

With the proposed method and system, we found that the InCC was not increased until the light intensity exceeds a certain value, and the increased InCC gradually returns to baseline when the pulse light is removed. At the same time, the induced increment of InCC by 453 nm light did not change significantly within the range of light intensity from 5.3 to 107.1 mJ/cm^2. This response characteristic of yes or no is similar to that of nerve impulse. In addition, the irritation of test light only lasts for 300 µs, while the intracellular high concentration of calcium can be maintained for 1-20 s. This inconsistency in response time, as well as the shielding effect of the optical filter, can exclude the interference possibility from light leakage. Therefore, the experiment results and detection methods used here are effective and reliable.

4.2. Quantitative measurement advantage for effective/minimum light parameters

Using the method we developed, unknown photoresponse and light regulation parameters on target cells can be found. Table 1 shows many different optical parameters of stimulated lights in vivo auditory nerve in reported research. And in this paper, another photoresponse band is found for SGCs, either. The increase in InCC confirmed that the mono-pulse blue light (453 nm, 300 µs) could induce the signal transduction activity of natural SGCs, whereas the similar near infrared light (810 nm, 300 µs) was difficult to induce. In other words, the natural SGC is more sensitive to blue light on mono-pulse light modulation. We also found that blue light repeatedly induced SGCs' InCC activity over a wide range of light intensity (5.3-107.1 mJ/cm^2), which suggests that blue light stimulation had no significant damage to SGCs. Therefore, by using quantitative contrast detection method, more photosensitive response characteristics and more efficient photoregulation parameters of target cells can be found. Of course, whether the increased InCC can further induce nerve impulses of natural SGCs, and whether the long-term light stimulation is safe and effective still need to be further evaluated by in vivo light stimulation experiments.

4.3. Further analysis on SGCs' light-regulation mechanism

At present, most researchers believe that light-induced auditory nerve conduction mainly results from photothermal effects [3,5,29], and studies have confirmed that SGCs and vestibular ganglion cells have thermosensitive ions channel, TRPV4 [30,31]. But this photothermal mechanism is hard to explain our findings in this paper, because we have systematically measured the photothermal effect of multi-band pulse lights, and found the photothermal effect of blue light (453 nm) was comparable to that of near-infrared light (810 nm) [32]. However, the increase of the InCC occurs only in the irradiation of the blue pulse light, while the 810 nm light with the similar photothermal effect fails to induce this change of InCC, as shown in Fig. 6(b).

We further measured the photomechanical pressure effect caused by the two pulsed lights [33]. In the experiment, a thin-film pressure sensor was used to collect the pressure effect data

Biomedical Optics EXPRESS

Table 1. The Optical Stimulation Parameters in Auditory Nerves

Subject	In vivo / vitro	Wavelength	Pulse width & Frequency	Energy Density	Reference
Cat and guinea pig cochleae	In vivo	1850nm 1860nm	100 µs @ 100Hz	20 µJ/pulse	(2018, Xu, Yingyue et al. [1])
Spiral ganglion neurons in the guinea pigs of cochlea	In vivo	980nm	20 µs - 500 µs @ -	10 to 102 mJ/cm^2	(2017, Wang J.X. et al. [21])
Spiral ganglion neurons in the guinea pigs of cochlea	In vivo	810nm	20 µs −300 µs @ 11Hz	20.4 to 1.02 × 103 mJ/cm^2	(2016, Wang J.X. et al. [22])
Basilar membrane of guinea pigs	In vivo	532nm	10 ns @ 10Hz	0.6 to 23µJ/pulse	(2009, Wenzel G. I. et al. [28])
Cochlear spiral ganglion cells of the gerbil	In vivo	1855nm	35 µs - 1 ms @ 13Hz	5.29 ± 0.6 mJ/cm^2	(2007, Agnella D. Izzo et al. [7])
Cochlear spiral ganglion cells of the gerbil	In vivo	2120nm	250 µs @ 2Hz	18 ± 3 mJ/cm^2	(2006, Agnella D. Izzo et al. [4])

(*i.e.* amplitude), meanwhile the pulse light with the similar optical energy density and same pulse width (*i.e.* 56.6 mJ/cm^2 and 300 µs), mean the pulse light with the similar optical energy. The results are shown in Fig. 8. It was found that the corresponding pressure produced by the mono-pulse light is significantly different, that is, the pressure produced by the pulse blue light is nearly 5 times larger than that of the 810 nm light. Therefore, it is deduced that the combination of the specific band (453 nm) and its photomechanical effect can be the main reason for this results.

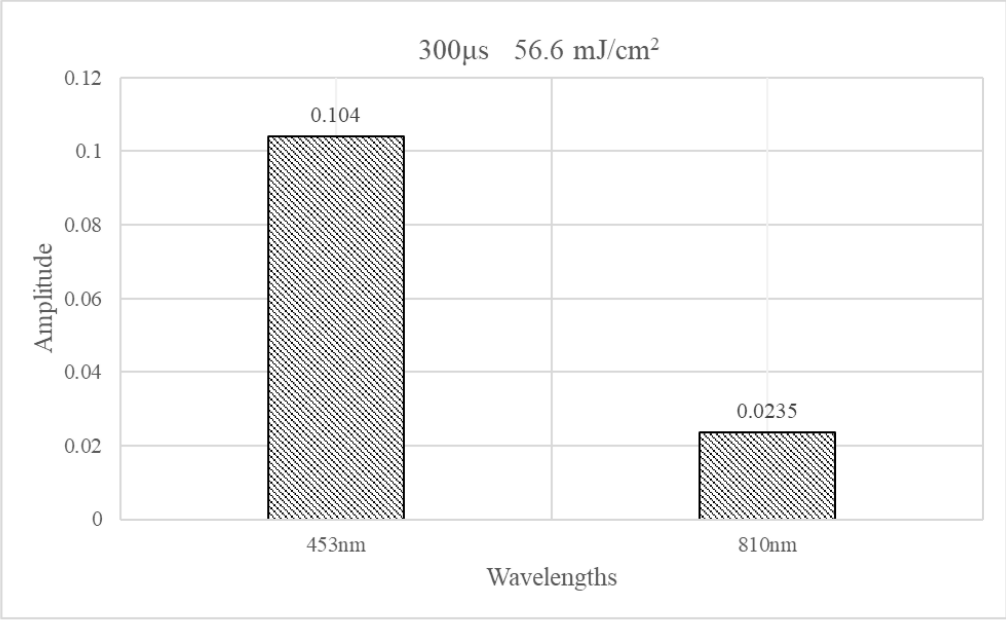

Fig. 8. The result of the mono-pulse photomechanical pressure with different wavelengths at the same light parameters.

Biomedical Optics EXPRESS

It can be seen from above discussions, the proposed screening and detection method does not depend on the type of cells or the bands of test light. It is applicative in the study of light-regulation parameters of other cells in vitro. Furthermore, since the system can simultaneously detect a large number of target cells, its detection throughput is higher and its operability is better, compared to those of the electrophysiological techniques like patch clamp. In addition, photothermal effect has the risk of biological thermal damage. As a result, in the study of photo-induced regulation of neural activity, it is necessary to constrain the light intensity [34]. The different changes in InCC in natural SGCs under the two times stimulus of 453 nm light in Fig. 6(b) may be related to the thermal damage from too higher irradiation of 810 nm light in the intermediate stage. This shows that quantitative detection and analysis on cell photosensitive response is very necessary.

5. Conclusion

In order to screen systematically whether target cells have a photosensitive effect and further to detect the optimal effective and/or efficient regulation parameters, this paper proposes a system and method to detect the real-time changes of InCC of target cells in vitro under the quantitative irradiation of different test lights. The method uses adjustable parameter pulse lights and calcium imaging to observe photosensitive responses of a large number of target cells. As presentation target object, natural mice SGCs were experimented by the method. The results showed that the blue pulse light (453 nm, 300 μs) causes obvious increase of InCC of the SGCs, while the same parameter's pulse light of 810 nm cannot effectively induce the evident increase of the InCC. This study suggests a new and higher efficient candidate light of 453 nm for light-regulation of natural SGCs, and at the same time, we detected its minimum effective stimulation energy for single pulse width of 300 μs is 5.3 mJ/cm^2. The detection study on natural SGCs in vitro proves that the proposed method is useful for discovering the specific photosensitive effects of natural cells and will promote the photoregulation technology development in biomedical engineering.

Funding. Natural Science Foundation of Shandong Province (ZR2020QA063, ZR2021MF065, ZR2021ZD40); National Natural Science Foundation of China (12204273).

Acknowledgments. The authors very gratefully acknowledge Ming Xia, Chengcheng Liu, and Xiulin Zhang of the Electrophysiology Laboratory of the Second Hospital of Shandong University for technical assistance in use and debugging of the experimental equipment during electrophysiological experiments, and for giving us many useful suggestions in the research.

Disclosures. The authors declare no conflicts of interest.

Data availability. Data underlying the results presented in this paper are not publicly available at this time but may be obtained from the authors upon reasonable request.

References

1. Y. Xu, N. Xia, M. Lim, X. Tan, M. H. Tran, E. Boulger, F. Peng, H. Young, C. Rau, A. Rack, and C.-P. Richter, "Multichannel optrodes for photonic stimulation," Neurophotonics **5**(04), 1 (2018).
2. X. Tan, S. Rajguru, H. Young, N. Xia, S. R. Stock, X. Xiao, and C.-P. Richter, "Radiant energy required for infrared neural stimulation," Sci. Rep. **5**(1), 13273 (2015).
3. J. Wells, C. Kao, K. Mariappan, J. Albea, E. D. Jansen, P. Konrad, and A. Mahadevanjansen, "Optical stimulation of neural tissue in vivo," Opt. Lett. **30**(5), 504–506 (2005).
4. A. D. Izzo, C.-P. Richter, E. D. Jansen, and J. T. Walsh, "Laser stimulation of the auditory nerve," Lasers Surg. Med. **38**(8), 745–753 (2006).
5. C.-P. Richter and X. Tan, "Photons and neurons," Hear. Res. **311**, 72–88 (2014).
6. A. D. Izzo, J. Wells, M. Bendett, and C. P. Richter, "Laser stimulation of the auditory system at 1.94μm and microsecond pulse durations," Biophys. J. **94**(8), 3159–3166 (2008).
7. A. D. Izzo, J. T. Walsh, E. D. Jansen, M. Bendett, J. Webb, H. Ralph, and C.-P. Richter, "Optical parameter variability in laser nerve stimulation: a study of pulse duration, repetition rate, and wavelength," IEEE Trans. Biomed. Eng. **54**(6), 1108–1114 (2007).
8. J. Wells, C. Kao, E. D. Jansen, P. Konrad, and A. Mahadevan-Jansen, "Application of infrared light for in vivo neural stimulation," J. Biomed. Opt. **10**(6), 064003 (2005).
9. J. Wells, P. Konrad, C. Kao, E. D. Jansen, and A. Mahadevan-Jansen, "Pulsed laser versus electrical energy for peripheral nerve stimulation," J. Neurosci. Methods **163**(2), 326–337 (2007).

Biomedical Optics EXPRESS

10. H. Ye and M. Fussenegger, "Optogenetic medicine: synthetic therapeutic solutions precision-guided by light," Cold Spring Harbor Perspect. Med. **9**(9), a034371 (2019).
11. Q. Luo, "A brief introduction to biophotonic techniques and methods," Sci. China: Life Sci. **63**(12), 1771–1775 (2020).
12. H. Bansal, N. Gupta, and S. Roy, "Theoretical analysis of low-power bidirectional optogenetic control of high-frequency neural codes with single spike resolution," Neuroscience **449**, 165–188 (2020).
13. O. Yizhar, L. E. Fenno, T. J. Davidson, M. Mogri, and K. Deisseroth, "Optogenetics in neural systems," Neuron **71**(1), 9–34 (2011).
14. R. T. Richardson, M. R. Ibbotson, A. C. Thompson, A. K. Wise, and J. B. Fallon, "Optical stimulation of neural tissue," Healthcare Technology Letters **7**(3), 58–65 (2020).
15. N. Xia, X. Tan, Y. Xu, W. Hou, T. Mao, and C.-P. Richter, "Pressure in the cochlea during infrared irradiation," IEEE Trans. Biomed. Eng. **65**(7), 1575–1584 (2018).
16. C. Grienberger and A. Konnerth, "Imaging calcium in neurons," Neuron **73**(5), 862–885 (2012).
17. X. Tan, I. Jahan, Y. Xu, S. Stock, C. C. Kwan, C. Soriano, X. Xiao, J. Garcia-Anoveros, B. Fritzsch, and C. P. Richter, "Auditory Neural Activity in Congenitally Deaf Mice Induced by Infrared Neural Stimulation," Sci. Rep. **8**(1), 388 (2018).
18. B. Jiang, W. Hou, N. Xia, F. Peng, X. Wang, C. Chen, Y. Zhou, X. Zheng, and X. Wu, "Inhibitory effect of 980-nm laser on neural activity of the rat's cochlear nucleus," Neurophotonics **6**(03), 1 (2019).
19. C.-P. Richter, R. Bayon, A. D. Izzo, M. Otting, E. Suh, S. Goyal, J. Hotaling, and J. T. Walsh, "Optical stimulation of auditory neurons: Effects of acute and chronic deafening," Hear. Res. **242**(1-2), 42–51 (2008).
20. S. M. Rajguru, A. I. Matic, A. M. Robinson, A. J. Fishman, L. E. Moreno, A. Bradley, I. Vujanovic, J. Breen, J. D. Wells, M. Bendett, and C.-P. Richter, "Optical cochlear implants: Evaluation of surgical approach and laser parameters in cats," Hear. Res. **269**(1-2), 102–111 (2010).
21. L. Tian, J. Wang, Y. Wei, J. Lu, A. Xu, and M. Xia, "Short-wavelength infrared laser activates the auditory neurons: comparing the effect of 980 vs. 810 nm wavelength," Lasers Med. Sci. **32**(2), 357–362 (2017).
22. J. Wang, L. Tian, J. Lu, M. Xia, and Y. Wei, "Effect of shorter pulse duration in cochlear neural activation with an 810-nm near-infrared laser," Lasers Med. Sci. **32**(2), 389–396 (2017).
23. J. Wang, J. Lu, C. Li, L. Xu, X. Li, and L. Tian, "Pulsed 980 nm short wavelength infrared neural stimulation in cochlea and laser parameter effects on auditory response characteristics," BioMed Eng OnLine **14**(1), 89 (2015).
24. B. Liu, R. Chen, J. Wang, Y. Li, C. Yin, Y. Tai, H. Nie, D. Zeng, J. Fang, J. Du, Y. Liang, X. Shao, J. Fang, and B. Liu, "Exploring neuronal mechanisms involved in the scratching behavior of a mouse model of allergic contact dermatitis by transcriptomics," Cell. Mol. Biol. Lett. **27**(1), 16 (2022).
25. H. Dana, Y. Sun, B. Mohar, B. K. Hulse, A. M. Kerlin, J. P. Hasseman, G. Tsegaye, A. Tsang, A. Wong, R. Patel, J. J. Macklin, Y. Chen, A. Konnerth, V. Jayaraman, L. L. Looger, E. R. Schreiter, K. Svoboda, and D. S. Kim, "High-performance calcium sensors for imaging activity in neuronal populations and microcompartments," Nat. Methods **16**(7), 649–657 (2019).
26. G. Grynkiewicz, M. Poenie, and R. Y. Tsient, "A new generation of Ca^{2+} indicators with greatly improved fluorescence properties," J. Biol. Chem. **260**(6), 3440–3450 (1985).
27. T. Lan, Z. Ming, H. Houze, L. Zhaoyang, and L. Xiaoshan, "A multi-band pulse laser control system and method via parameter adjustment based on look-up table.," P.R.C patent CN202210789664.5 (October 11, 2022).
28. G. I. Wenzel, S. Balster, K. Zhang, H. H. Lim, U. Reich, O. Massow, H. Lubatschowski, W. Ertmer, T. Lenarz, and G. Reuter, "Green laser light activates the inner ear," J. Biomed. Opt. **14**(4), 044007 (2009).
29. M. G. Shapiro, K. Homma, S. Villarreal, C.-P. Richter, and F. Bezanilla, "Infrared light excites cells by changing their electrical capacitance," Nat. Commun. **3**(1), 736 (2012).
30. E. S. Albert, J. M. Bec, G. Desmadryl, K. Chekroud, C. Travo, S. Gaboyard, F. Bardin, I. Marc, M. Dumas, G. Lenaers, C. Hamel, A. Muller, and C. Chabbert, "TRPV4 channels mediate the infrared laser-evoked response in sensory neurons," J. Neurophysiol. **107**(12), 3227–3234 (2012).
31. J. N. Barrett, S. Rincon, J. Singh, C. Matthewman, J. Pasos, E. F. Barrett, and S. M. Rajguru, "Pulsed infrared releases Ca^{2+} from the endoplasmic reticulum of cultured spiral ganglion neurons," J. Neurophysiol. **120**(2), 509–524 (2018).
32. J. Xu, M. Zeng, X. Xu, J. Liu, X. Huo, D. Han, Z. Wang, and L. Tian, "A Micron-Sized Laser Photothermal Effect Evaluation System and Method," Sensors **21**(15), 5133 (2021).
33. X. S. Lu, L. Tian, and W. Liu, "Micron-sized multispectral multi-parameters pulse light photo-induced pressure measurement system and method.," Patent Office of the People's Republic of China patent CN202111563904 (April 5, 2022).
34. S. F. Owen, M. H. Liu, and A. C. Kreitzer, "Thermal constraints on in vivo optogenetic manipulations," Nat. Neurosci. **22**(7), 1061–1065 (2019).